Alignment of Plate-Like Particles in a Colloidal Dispersion under Flow in a Uniform Pipe Studied by High-Energy X-ray Diffraction

ARTICLE *in* LANGMUIR · DECEMBER 2010

Impact Factor: 4.46 · DOI: 10.1021/la103537y · Source: PubMed

4 AUTHORS, INCLUDING:

Junaid Qazi
The University of Calgary
12 PUBLICATIONS **73** CITATIONS
SEE PROFILE

Jon P Wright
European Synchrotron Radiation Facility
163 PUBLICATIONS **1,623** CITATIONS
SEE PROFILE

J. K. Cockcroft
University College London
84 PUBLICATIONS **1,208** CITATIONS
SEE PROFILE

Langmuir
Article
pubs.acs.org/Langmuir

Alignment of Plate-Like Particles in a Colloidal Dispersion under Flow in a Uniform Pipe Studied by High-Energy X-ray Diffraction

S. Junaid S. Qazi,*[,†,‡] Adrian R. Rennie,[‡] Jonathan P. Wright,[§] and Jeremy K. Cockcroft[∥]

[‡]*Department of Physics and Astronomy, Uppsala University, Box 516, S-751 20 Uppsala, Sweden,* [§]*European Synchrotron Radiation Facility, BP 220X, F-38 043 Grenoble Cedex, France, and* [∥]*Department of Chemistry, University College London, 20 Gordon Street, London, WC1H 0AJ, United Kingdom.* [†]*On study leave from COMSATS Institute of Information Technology, Pakistan.*

Received September 3, 2010. Revised Manuscript Received November 5, 2010

High-energy angle-dispersive X-ray diffraction has been used to study the alignment of colloidal suspension of kaolinite particles in water as they flow along a pipe. X-rays with energies above 25 keV have a major advantage, as they can penetrate through thick samples and walls of containers and permit investigation of samples under realistic flow conditions. As an example of the method, flow through a circular cross-section pipe with an internal diameter of 5 mm has been studied: this is typical of industrial applications. The angular distribution of intensities of peaks in the diffraction pattern as a function of the location of the pipe in the X-ray beam provides information about the alignment of particles under flow. Order parameters have been calculated to describe the alignment and direction of orientation. It is observed that the particles align in the direction of flow with their flat faces parallel to the flow. The experimental results are compared with the calculations of the local strain rate that help to explain the onset of alignment of the particles.

Introduction

Materials such as pastes and colloidal dispersions exhibit interesting behavior under flow. Rheological parameters such as viscosity, storage modulus, and yield stress depend strongly on particle concentration, deformation rate and strain history of the sample, and the shape and interaction of the particles.[1] Rheology of pastes[2] and the changes in structure that occur in colloidal systems under shear flow have been reviewed recently.[3,4] Many studies have involved spherical colloidal particles under flow. For example, small-angle neutron scattering has been used to reveal changes from a disordered crystal to sliding layers in a sample of charge-stabilized polystyrene latex.[5] Formation of aligned strings under shear in sterically stabilized dispersions of poly(methyl methacrylate) particles have been reported in a study that used low-angle light scattering.[6] The sterically stabilized latex approximates to particles with hard-sphere interactions, and such systems have been extensively studied by computer simulation. The experimentally observed structures closely resembled the structures found in the Brownian dynamics simulations of Heyes and Melrose.[7] When spherical particles are dispersed in a solution of surfactant that contains micelles a variety of structures have been reported as a function of shear rate.[8] String-like structures were seen at low shear rates and a two-dimensional planar crystal formed at high shear rates. Flow processing has significant importance in the formation of colloidal microstructures in finished products such as processed foods.[9] Understanding and controlling the structure of materials as they flow is thus of fundamental importance for a wide range of process industries.

Anisotropic colloidal particles are used in many applications as reinforcing filler particles in polymeric materials, in coatings for paper products, as lubricants, and in a range of domestic and personal care products. Plate-like anisotropic colloidal dispersions have shown orientational ordering. Kaolinite (a layered silicate with nominal formula $Al_2Si_2O_5(OH)_4$) dispersions have been studied under pipe flow using energy-dispersive X-ray diffraction.[10,11] Dispersions of clays can also display complex gelling behavior, and such materials have been studied by small-angle neutron scattering.[12] Measurements of orientation by small-angle scattering of either X-rays or neutrons require particles that can be resolved, and this will usually impose an upper limit of a few hundred nanometers. For such samples to align strongly, the viscosity would have to be high, for example, with high particle concentrations. Alternatively, very high strain rates are required. In contrast, diffraction measurements can work with a wide range of particle sizes and can provide a full quantitative determination of the orientation distribution. For example, a system of monodisperse plates made by the stabilization of nickel hydroxide with sodium polyacrylate has been investigated using small-angle neutron scattering and neutron diffraction under shear flow.[13] The diffraction measurements showed the transition from a columnar phase to sliding uncorrelated layers as the shear

*Contact author: S. Junaid S. Qazi. Telephone: + 46 18 471 3522. E-mail: Junaid.Qazi@fysik.uu.se.

(1) Goodwin, J. W.; Hughes, R. W. *Rheology for Chemists — an Introduction*; Royal Society of Chemistry: Cambridge, 2000.
(2) Coussot, P. *Soft Matter* **2007**, *3*, 528–540.
(3) Vermant, J.; Solomon, M. J. *J. Phys.: Condens. Matter* **2005**, *17*, R187–R216.
(4) Malkin, A. Ya.; Semakov, A. V.; Kulichikhin, V. G. *Adv. Colloid Interface Sci.* **2010**, *157*, 75–90.
(5) Ashdown, S.; Markovic, I.; Ottewill, R. H.; Lindner, P.; Oberthür, R. C.; Rennie, A. R. *Langmuir* **1990**, *6*, 303–307.
(6) Clarke, S. M.; Ottewill, R. H.; Rennie, A. R. *Adv. Colloid Interface Sci.* **1995**, *60*, 95–118.
(7) Heyes, D. M.; Melrose, J. R. *J. Non-Newtonian Fluid Mech.* **1993**, *46*, 1–25.
(8) Pasquino, R.; Snijkers, F.; Grizzuti, N.; Vermant, J. *Langmuir* **2010**, *26*, 3016–3019.
(9) Walkenström, P.; Hermansson, A. M. *Curr. Opin. Colloid Interface Sci.* **2002**, *7*, 413–418.
(10) Barè, S.; Cockcroft, J. K.; Colston, S. L.; Jupe, A. C.; Rennie, A. R. *J. Appl. Crystallogr.* **2001**, *34*, 573–579.
(11) Rennie, A. R.; Bare, S.; Cockcroft, J. K.; Jupe, A. C. *J. Colloid Interface Sci.* **2006**, *293*, 475–482.
(12) Ramsay, J. D. F.; Lindner, P. *J. Chem. Soc. Faraday Trans* **1993**, *89*, 4207–4214.
(13) Brown, A. B. D.; Rennie, A. R. *Phys. Rev. E* **2000**, *62*, 851–862.

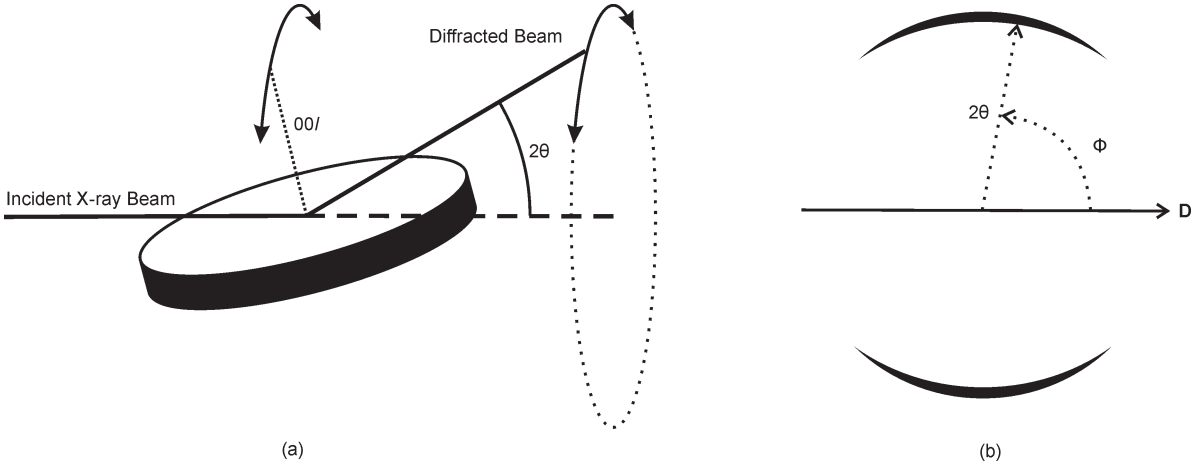

Figure 1. (a) Schematic diagram of diffraction from a single-crystal plate-like particle. The 001 diffraction peak is in a unique direction that can be related to the orientation of the particle. The distribution of the 001 peak intensity for an assembly of particles is thus simply related to the distribution of particle orientations. (b) Schematic diagram of diffracted intensity measured on a two-dimensional detector from a distribution of alignment about a single direction, **D**, is shown. The width of the peak as a function of the azimuthal angle, Φ, depends upon the distribution of the plate normals.

rate increased to the point where noticeable shear thinning is observed.

Despite this widespread interest in the structural changes induced by flow in concentrated colloidal dispersions, only a limited range of techniques is available to study their structure and orientation. Optical birefringence has been used[14] but is difficult to apply to concentrated samples and provides a single average measure of the orientation distribution. Small-angle neutron scattering has been used for studies for shear[15] and elongational[16,17] flow for both particulate and self-assembled colloids. This is easy to apply to a wide range of sample environments, and the scattering data contain information about correlations between particles, as well as their shape and orientation. This can make data analysis complicated. Scattering techniques have been used for a study of a range of clay dispersions and composites. A laboratory X-ray source could provide only limited data on the flow of a dispersed kaolinite.[18] Smaller clay particles such as laponites have been more widely studied by small-angle X-ray scattering.[19] Composites and mixtures of clay with polymers have also been a focus of recent interest.[20,21] Nuclear magnetic resonance can be used to measure anisotropy in flowing materials. However, there are severe restrictions of geometry, and it will usually provide just one average measurement of the orientation. This method has been applied, for example, to a variety of polymers and liquid crystals.[22] Magnetic resonance imaging has also been reported, but spatial resolution is limited.[23,24]

Diffraction techniques can provide complete information about the orientation in polycrystalline samples. This method has been applied to colloidal dispersions of particles. Energy-dispersive X-ray diffraction[10,11] and neutron diffraction[25,26] have also been used previously to study the alignment of kaolinite particles in flow fields. Neutron beams can penetrate thick and concentrated samples, but the spatial resolution is low because of the low incident flux and consequent larger beam size.

We have developed a new technique that exploits high-energy angle-dispersive synchrotron X-ray diffraction to study dispersions of crystalline particles under flow. In this paper, we present a study of the flow of a kaolinite dispersion in a straight pipe. Data for orientation of particles are compared with simple fluid mechanics simulations.

Concepts and Experimental Principles

Diffraction to Measure Orientation. Crystalline particles diffract X-rays when the angle, θ, between the incident beam and the separation of planes of atoms, d, in the crystal satisfies the Bragg condition for a given wavelength, $\lambda = 2d \sin \theta$. The distribution of orientation of crystals can be determined from the angular distribution of the diffracted intensity at a given scattering angle 2θ as shown in Figure 1a. Within a single plane, the orientation can be described in terms of a function $I(\Phi)$, where Φ is an azimuthal angle defined in terms of the axes defining the sample and its flow geometry as shown in Figure 1b.

Many anisotropic particles have an internal crystal structure that is correlated with the morphology of the particles. For example, kaolinite has a layered structure formed of alumino-silicate sheets. Its crystal structure and diffraction pattern are well-known.[27] In the case of disk-like particles, the orientation is conveniently described in terms of the direction of the line that is normal to the large face. The shape of kaolinite particles can be approximated as disks with a unique crystallographic normal described by Miller indices 00*l* parallel to the plate normal. The distribution of particle orientation is conventionally described with respect to a unique axis known as the director that is chosen with respect to the field that aligns the sample. The diffraction from a single plate has been shown schematically in Figure 1a. In the case of flow along a pipe in a single direction, it is convenient

(14) Schmidt, G.; Nakatani, A. I.; Han, C. C. *Rheol. Acta* **2002**, *41*, 45–54.
(15) Förster, S.; Konrad, M.; Lindner, P. *Phys. Rev. Lett.* **2005**, *94*, 017803–017804.
(16) Penfold, J.; Tucker, I. *J. Phys. Chem. B* **2007**, *111*, 9496–9503.
(17) Qazi, S. J. S.; Rennie, A. R.; Tucker, I.; Penfold, J. Manuscript in preparation.
(18) Jogun, S. M.; Zukoski, C. F. *J. Rheol.* **1999**, *43*, 847–871.
(19) Pignon, F.; Magnin, A.; Piau, J. M.; Cabane, B.; Lindner, P.; Diat, O. *Phys. Rev. E* **1997**, *56*, 3281–3289.
(20) Pujari, S.; Dougherty, L.; Mobuchon, C.; Carreau, P. J.; Heuney, M.-C.; Burghardt, W. R. *Rheol. Acta* **2010**, DOI 10.1007/s00397-010-0492-3
(21) Dykes, L. M. C.; Torkelson, J. M.; Burghardt, W. R.; Krishnamoorti, R. *Polymer* **2010**, *51*, 4916–4927.
(22) Siebert, H.; Ouijada-Garrido, I.; Vermant, J.; Noirez, L.; Burghardt, W. R.; Schmidt, C. *Macromol. Chem. Phys.* **2007**, *208*, 2161–2172.
(23) Callaghan, P. T. *Curr. Opin. Colloid Interface Sci.* **2006**, *11*, 13–18.
(24) Callaghan, P. T. *Rheol. Acta* **2008**, *47*, 243–255.
(25) Clarke, S. M.; Rennie, A. R.; Convert, P. *Europhys. Lett.* **1996**, *35*, 233–238.
(26) Brown, A. B. D.; Clarke, S. M.; Convert, P.; Rennie, A. R. *J. Rheol.* **2000**, *44*, 221–233.
(27) Brindley, G. W.; Brown, G. *Crystal Structures of Clay Minerals and their X-ray identification*; Mineralogical Society: London, 1984.

to define Φ as the angle between the unique flow direction and the single axis that describes the orientation of a particle that is the disk normal.

Use of Synchrotron Radiation. The absorption of X-rays decreases with increasing photon energy that corresponds to decreasing wavelength. Short wavelength X-rays are advantageous, as they penetrate thick samples and containers. This enables studies of samples in containers that resist the stresses imposed by the flow. The optimal wavelength can be chosen as a synchrotron provides a white spectrum. The choice of wavelength is a balance between the intensity of Bragg diffraction that increases with wavelength as λ^3 and the absorption that increases strongly with increasing wavelength. This choice will depend on the thickness of the sample and material of the container. A further advantage of high-energy X-rays is that the beam can be focused to a small size by refractive lenses.[28]

Modern synchrotron radiation sources produce highly collimated bright X-ray beams. These characteristics of the radiation allow measurements from small sample volumes or defined small sample regions within large samples. If a high-energy beam is used, most useful Bragg diffraction peaks will occur at small scattering angles.

Flow Geometry. In a scattering experiment, the sample volume is defined by the intersection of the incident beam with the sample. For a single-point detector, this volume would be further restricted by the volume of the sample as seen by the detector. In both cases, the volume may be further defined by the use of slits or pinholes as collimation before and after the sample. For low-angle diffraction, the shape of the scattering volume will always be elongated in a direction parallel to the incident beam. The position along this direction could be resolved in principle by the use of a tomographic scan in which the sample cell is positioned in different orientations within the incident beam. In practice, this is very difficult even for flow fields with high symmetry, since the transmission and scattering vary in different directions.[23] It is therefore attractive to look at simple systems with high symmetry for initial studies. In this work, we have chosen a cylindrical pipe that has a circular symmetry. Although there are different path lengths across the pipe, which range from zero up to the diameter of the pipe, the effects of absorption and sample volume can be calculated.

A further symmetry related factor in the design of experiments is the anisotropy of the crystalline particles that are studied. For a crystalline particle that approximates a disk, the unique orientation is described by the normal to the plane of the disk. For a needle-like particle, the unique direction will be the cylindrical axis itself. Under shear flow, the long dimension of both of these particles tends to align in the flow direction. For experiments that are concerned with the alignment of anisotropic particles, the measurements are primarily aimed at determining the distribution of orientations of unique directions of particles with respect to the principle directions of the aligning stress field. For approximately cylindrical disks in a cylindrical pipe, an ideal experiment would aim to determine the distribution of the plate normals with respect to the cylindrical axis at individual points within the pipe. In practice, experiments will always measure diffracted intensity from a line that passes through the sample. For simplicity, we have chosen that the beam passes normal to the axis of the pipe and this provides orientational information that is averaged along chords in the absence of collimation after the sample in a low-angle diffraction experiment.

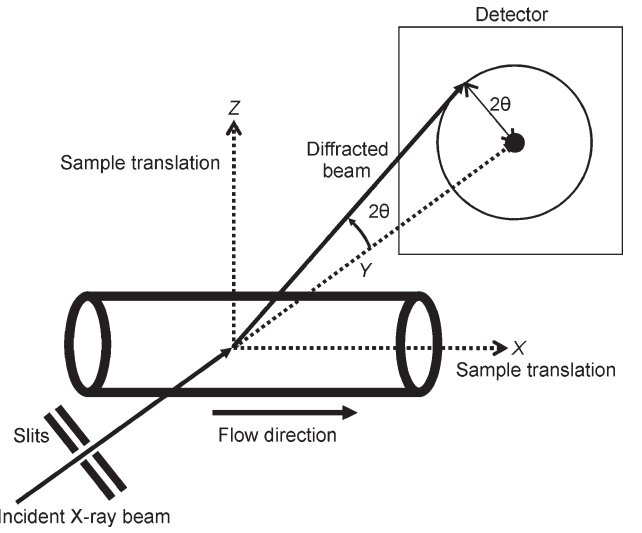

Figure 2. Schematic diagram of the X-ray diffraction experiment using an area detector for angle-dispersive measurements. The combination of slits and lenses provided a spot size of 20 μm × 20 μm. The sample was translated along horizontal and vertical directions to provide a two-dimensional map of alignment of plate-like particles under flow.

Advantages of Two-Dimensional Detectors. A two-dimensional area detector can be used to simultaneously measure data for a range of diffraction angles, 2θ, as well as a range of azimuthal angles, Φ. Suitable detectors are available for angle-dispersive measurements. In contrast, energy-dispersive experiments require large cooled-crystal detectors that can measure only at single scattering angle. Although an early attempt at an angle-dispersive experiment used an image plate,[10] charge-coupled device (CCD) detectors have advantages in providing rapid readout of quantitative data. Collimation between the sample and the detector cannot be used without restricting severely the range of scattering angles and speed of data acquisition for any area detector. A further advantage of an area detector is the capability to simultaneously measure a range of diffraction peaks. This can be exploited in studies of mixtures of different materials, as well as provide information about various components of orientation distributions that would be obtained from different crystallographic planes in particles.

When an area detector is placed normal to the incident beam and if the axis of the pipe is placed horizontal and normal to the incident beam, then the variation in intensity at a particular scattering angle, 2θ, with azimuthal angle, Φ, on the detector is a convenient measure of orientation distribution as shown schematically in Figure 1b. This is the geometry used in the experiments described in this paper.

Experimental Methods

Sample Preparation. An aqueous colloidal dispersion was prepared by adding 8 wt % kaolinite in water (approximately 3 vol %). The dried kaolinite was used as received from Sigma Aldrich, Germany. Light scattering and electron microscopy indicated that the diameter was dispersed in the range 1−2 μm and the thickness less than 0.1 μm. In water at pH 7, the faces of these plates dissociate to become positive, while the edges are negatively charged. Thus, edge to face attraction often causes flocculation and gelation in concentrated dispersions;[29] hence, a dispersion of kaolinite in water alone is not a stable colloidal system.

(28) Snigirev, A.; Snigireva, I.; Vaughan, G.; Wright, J.; Rossat, M.; Bytchkov, A.; Curfs, C. *J. Phys Conf. Ser.* **2009**, *186*, 012073.

(29) van Olphen, H. *An Introduction to Clay Colloid Chemistry*; Wiley: New York, 1963.

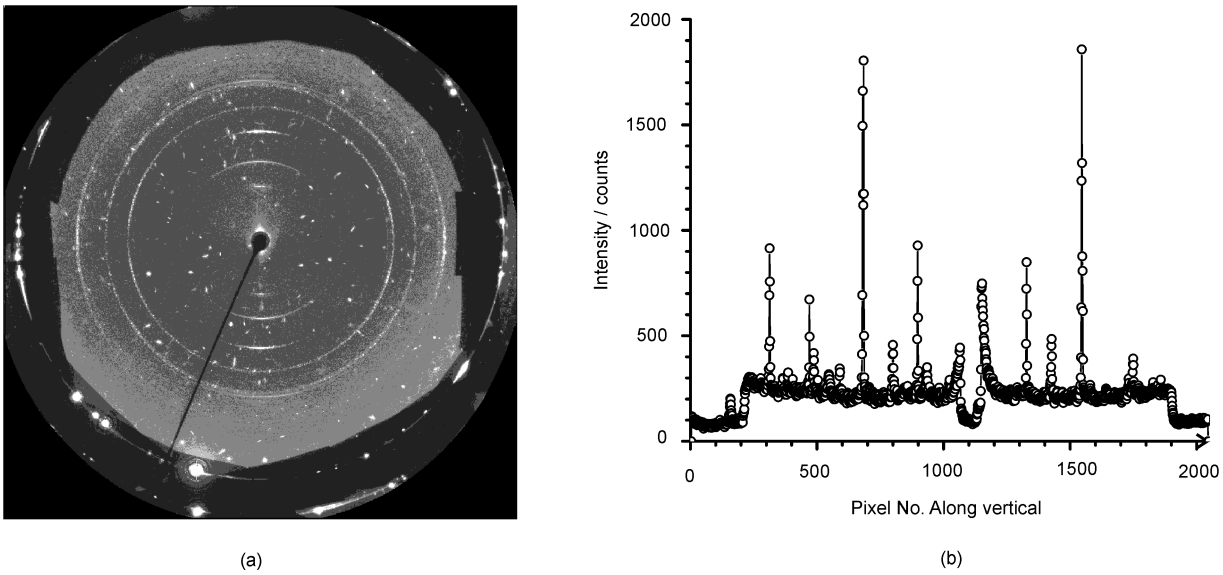

Figure 3. Raw diffraction data from the sample while flowing through the aluminum pipe are shown in (a) for a position near the wall at $X = 12$ mm, $Z = 2.35$ mm. Rings of diffraction from kaolinite are seen with preferred orientation for some Bragg peaks. Bright spots of diffraction from single grains of aluminum are also seen. In (b), the intensity is plotted as a function of pixel number for the vertical line at the middle of the detector.

To stabilize the particles against the flocculation, 0.5 wt % sodium polyacrylate with molecular mass of 4000 g mol^{-1} (N40, as provided by Ciba Chemicals, UK) was added. The detailed sample preparation method is described in a previous paper.[26]

Diffraction Experiments. Measurements were made on beamline ID11 at the European Synchrotron Radiation Facility (ESRF), Grenoble, France.[30] X-rays with energy of 46.8 keV were used that corresponds to a wavelength of 0.265 Å. The experimental arrangement is shown schematically in Figure 2, and further details are provided in the Supporting Information [S1(a)].

The small beam size on the sample was obtained using refractive lenses to focus the beam. The incident X-ray beam was perpendicular to the pipe and hence the flow direction. Aluminum was chosen for the pipe material in contrast to heavy metal alloys as it has a low absorption for X-rays, is easy to machine, and is structurally rigid. The cylindrical pipe (internal diameter of 5 mm and the wall thickness of 2.5 mm) was fixed on an $X-Y-Z$ translation stage that could move along horizontal (XY) and vertical (Z) directions. Images of diffracted intensity were obtained by moving the pipe thorough the beam along vertical and horizontal directions to build up maps of orientation. The volume flow rate was maintained at 26 cm^3 s^{-1} in the pipe for the experiments described below. Details of the data acquisition and the pump are provided in the Supporting Information [S1(b)] .

Data Reduction and Analysis

Description of Raw Images. A typical raw data set for a flowing sample at a position where strong alignment is observed near the wall of the pipe is shown in Figure 3a. The intensity along a vertical line through the center of the detector for this data set is plotted in Figure 3b, which shows diffraction peaks from the kaolinite. In Figure 3a, there are complete powder diffraction rings for kaolinite. Some rings show clear arcs of enhanced intensity that arise from preferential orientation of the anisotropic clay particles. The 001 peak for kaolinite is visible at a diffraction angle of 2.12°, and this corresponds to the known[27] d-spacing of 7.15 Å. The edges of the detector were masked with lead foil to attenuate the first (111) and second (200) diffraction peaks from aluminum that remain weakly visible as rings at the edge of the detector. Many bright diffraction spots are visible in the image. These arise from multiple diffraction from single-crystal grains of aluminum within the pipe that are of the order of the beam size used in these experiments. Several factors must be taken in to consideration when interpreting this type of data.

For quantitative analysis, it is important to make corrections for background scattering from the liquid, absorption from the walls of the container, and the scattering that arises from crystallites of aluminum in the pipe. The sample thickness varies from the edge of the pipe to the center because of its cylindrical geometry.

Data Reduction. The data were converted to $I(R, \Phi)$ using the diffraction rings to determine the coordinates of the center of the scattering on the detector where R is the radial distance for a given pixel. The diffraction angle 2θ is related to the distance $R_{2\theta}$ and the separation of the detector from the sample, L, by than $2\theta = R_{2\theta}/L$. Analysis of a specific diffraction ring at radius $R_{2\theta}$ involves background subtraction at each azimuthal angle, Φ, of the average intensity in two annuli at radii R_1 and R_2 inside and outside of the ring of interest as shown schematically in Figure 4. This provides the diffraction intensity from a specific Bragg peak of the clay particles without intensity contributions from the water or other smooth background.

The procedure to exclude single-crystal diffraction peaks that arise from the aluminum pipe in the data used for further analysis is described in the Supporting Information [S2].

Data Correction. The cross-section of a pipe is shown in the Figure 5a. The chord length, C, corresponds to the sample thickness for a particular position of measurement. The path length of aluminum in the beam also changes with the position of measurement. Two distinct factors arise from the changes in sample thickness and container thickness. The total scattered intensity of a diffraction peak on the detector is directly related to the amount of sample in the beam in the absence of multiple scattering. Normalization of the data by the chord length is required to compare frames of data measured at different positions in the pipe.

(30) ID11 beam line: http://www.esrf.eu/UsersAndScience/Experiments/StructMaterials/ID11/

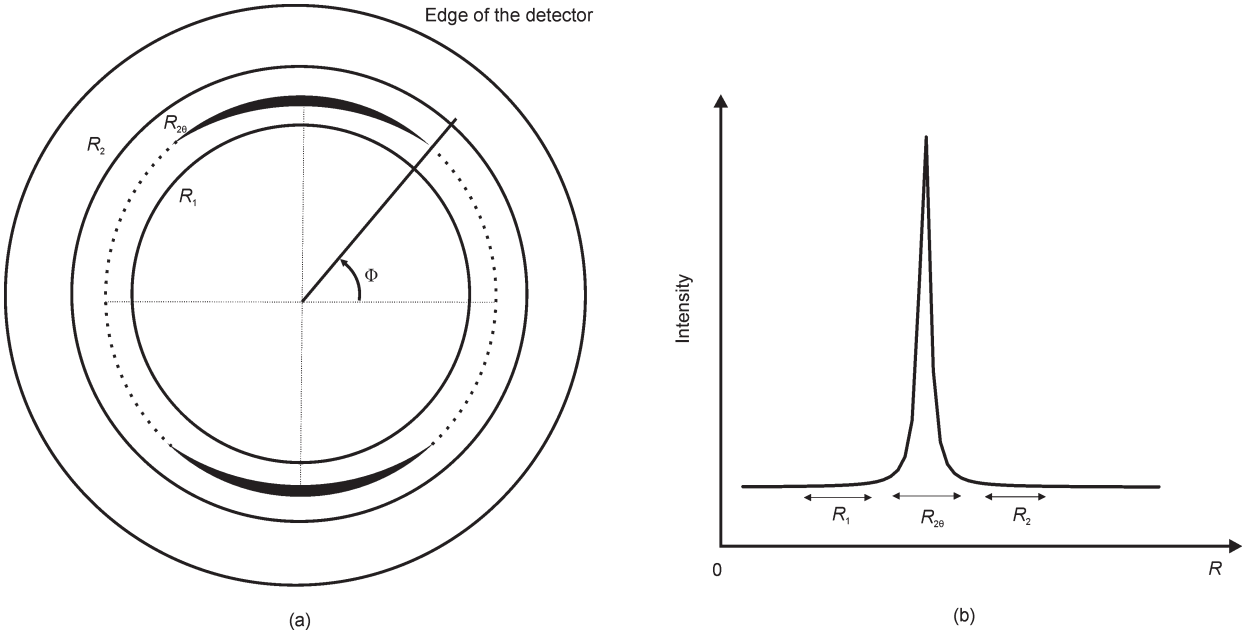

Figure 4. The background for each azimuthal angle Φ is subtracted by averaging the intensity of two annuli at radii R_1 and R_2, inside and outside of the diffraction ring at radius $R_{2\theta}$.

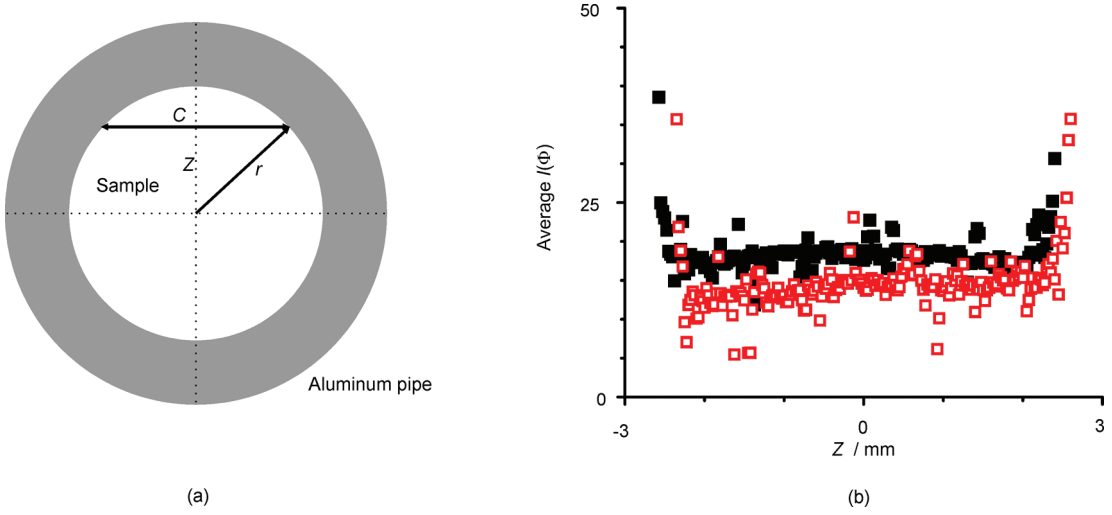

Figure 5. (a) Schematic cross-section of the pipe. The normalization for sample thickness for a beam that passes through the sample at height Z is determined by the chord length, C, and the internal radius of the pipe, r. (b) Chord-normalized intensity for the 001 diffraction averaged over all Φ. Data for a vertical scan across the pipe at the inlet (X = 12 mm) are shown as black solid squares and for a scan at the outlet (X = 42 mm) are shown as red open squares.

Figure 5b shows a plot of the chord-normalized intensity for the 001 kaolinite diffraction peak averaged over all Φ against the position Z across the pipe. The large flat region in the plot indicates that the chord normalization correctly accounts for the sample thickness. The data for both inlet and outlet positions are shown and are very similar, but the edges are offset slightly by about 0.2 mm because the pipe could not be mounted perfectly horizontally. The specific effects of the enhanced intensity at the walls arising from orientation will be discussed later.

As the sample cell was made of aluminum, the absorption for high-energy X-rays is not very large. For 46.8 keV X-ray photons, the calculated absorption coefficients for aluminum and for the sample are 1.07 cm^{-1} and 0.26 cm^{-1}, respectively. The sample thickness decreases and the aluminum thickness increases in a scan from the center to the edge of the pipe. These correlated changes when combined with the low absorption value of each component allow the net effect of absorption to be neglected. The flat lines in Figure 5b justify this approach.

Results and Discussion

Orientation Distributions from $I(\Phi)$. The alignment distribution of the normals of clay plates in the pipe is directly related to the intensity distribution of the 001 Bragg peak. Particles that are oriented with the normals to the large face parallel to the beam will not contribute to the 001 intensity on the detector. Particles with normals to the large faces that are perpendicular to the beam give rise to the 001 intensity. Although the Bragg angle is small (2.12°), it is not zero, and the diffraction condition is therefore satisfied for those particles with normals that are oriented slightly (1.06°) away from the perpendicular to the beam. In the absence of any preferred orientation, a uniform ring of diffraction intensity

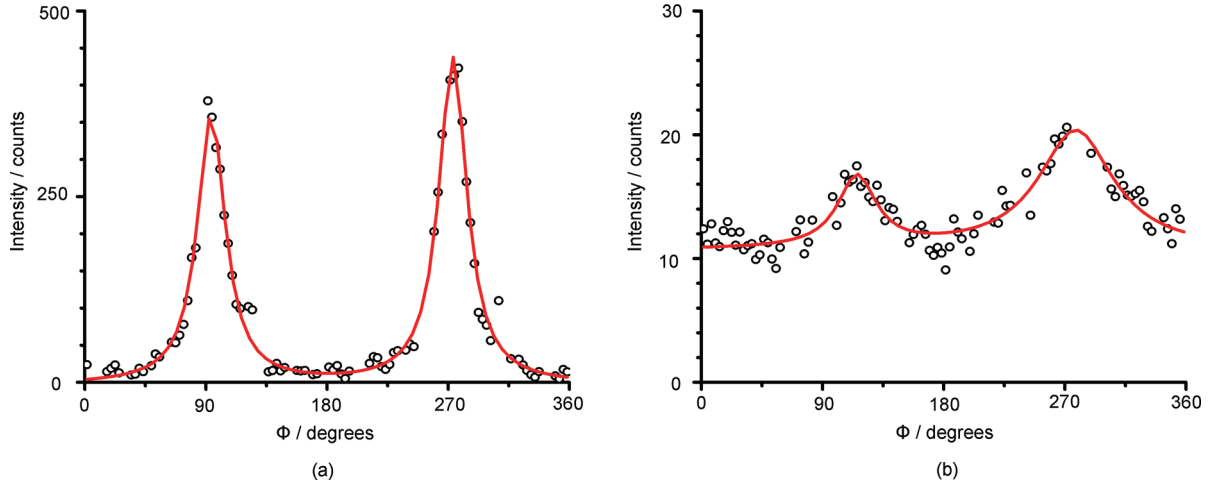

Figure 6. The red line is the Lorentzian fit to data points for 001 intensity peaks from clay particles (a) near the wall and (b) at the center of the pipe. Data points are obtained after background subtraction and masking.

would be observed. Clay particles with large faces that are parallel to the flow direction and to the beam satisfy the Bragg condition and give peaks at $\Phi = 90°$ and 270° with $\Phi = 0$ defined as the direction of the pipe.

The distribution of intensity with Φ directly measures the degree of alignment of the particles because of their unique direction of 001 crystal plane within each platelet. Figure 6 shows intensity distributions plotted against Φ for a position at the edge of the pipe and at the center. There are peaks in Figure 6a that extend from almost zero intensity to a high maximum. In contrast, at the center of the pipe (Figure 6b) the intensity is more uniform with a smaller modulation with Φ. The region at the center of the pipe has a large fraction of particles that are not aligned by the flow that give rise to an intensity that does not vary with Φ. The low average intensity results from this lack of alignment, as only a small fraction of the clay particles satisfy the Bragg condition. A small fraction of the particles is aligned by the flow, and this signal is superimposed on the uniform distribution.

Compared to the center of the pipe, near the walls a larger fraction of the particles is aligned with the normals to their large faces perpendicular to the flow. As the beam passes tangentially at the wall, a greater fraction of the particles satisfies the Bragg condition and does not diffract from a significant amount of the bulk of the sample. This explains the observation of strong, preferred orientation shown in Figure 6a and that the total intensity of diffraction from the particles is higher at the walls than at the center as shown in Figure 6b.

A major advantage of the diffraction technique is that it enables the orientation distribution functions to be determined completely. Different functions to describe the orientation distribution were tested. At the edge of the pipe, the best fits were obtained with Lorentzian functions as shown in the Figure 6a. The full width at half-maximum for each peak is 25° for this data. At the center of the pipe, it is difficult to distinguish among different forms of distribution functions, but the breadth of the distribution function is comparable to that seen at the edge. There is an asymmetry in the peak heights that consistently appeared in all diffraction patterns: this could be due to misalignment of the pipe that affects each diffraction pattern equally. The width of the peak is a measure of the breadth of the orientation distribution of the clay particles in Φ. A previous study[11] had described the orientation distribution as a Gaussian function over a large region at the center of a rectangular section pipe. However, the study had poor spatial resolution and was not able to determine the orientation distribution function close to the wall.

Table 1. Equations for the First Three Even Legendre Polynomials[31]

$P_0(x) = 1$
$P_2(x) = (3x^2 - 1)/2$
$P_4(x) = (35x^4 - 30x^2 + 3)/8$

The diffraction patterns measured at equivalent positions at both the inlet and the outlet ends of the pipe are very similar, and this shows that the particles do not change in orientation as they flow along the pipe.

Order Parameters for Flow. Analysis was extended to calculate order parameters to estimate the direction of the alignment as a function of azimuthal angle, Φ, with respect to the flow direction in kaolinite platelets. The distribution of intensity at a given scattering angle, 2θ, with respect to the azimuthal angle Φ can be described in terms of a sum of even Legendre polynomials. The equations for the first three even Legendre polynomials are listed in Table 1 and are shown graphically in the Supporting Information [S3]. As the pipe has mirror symmetry, only even functions are required to describe $I(\Phi)$. This is analogous to the description of a periodic function as a Fourier series. Such an expansion will generally require many terms, will require normalization coefficients for each polynomial, and may not converge rapidly; our discussion is therefore limited to the first-order parameter, S_2.

Theoretical models usually describe the extent of orientation of anisotropic particles in terms of order parameters that are weighted averages of the orientation distribution.[32] For example, an order parameter S_2 can be calculated as the normalized average $\langle P_2(x)\ I(\Phi)\rangle/\langle I(\Phi)\rangle$, where x is conventionally cos Φ and Φ is the angle between the unique axis of each particle and the director that defines the alignment. A perfectly aligned sample would then have an order parameter $S_2 = 1$, and a distribution that has no preferential orientation has $S_2 = 0.25$ as can be seen readily from Figure S1 in the Supporting Information. Order parameters can be calculated with respect to a single selected director. If the plate-like kaolinite particles align with their long dimension parallel to the flow direction, then they would have their 001 normal perpendicular to the axis of the cylindrical pipe

(31) Spiegel, M. R. *Mathematical Handbook of Formulas and Tables*; McGraw-Hill: New York, 1968; p 146.
(32) Chandrasekhar, S. *Liquid Crystals*; Cambridge University Press: Cambridge, 1980; p 42.

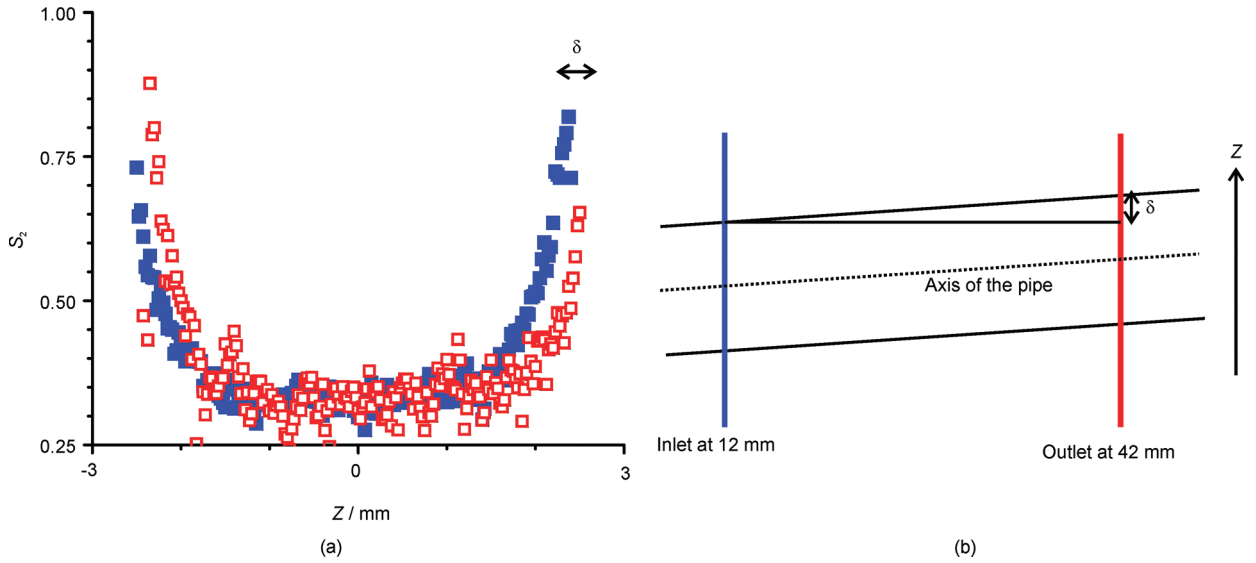

Figure 7. (a) Values of S_2 are plotted against the vertical position of the pipe at inlet (blue, filled squares) and the outlet (red, open squares). The positions are shown in (b). δ indicates a slight tilt in the pipe away from the horizontal that was found to be about 0.2 mm. The higher order is prominent near the walls.

and hence the flow direction. This makes it very convenient to select the director along the direction that is perpendicular to the axis of the pipe and the incident beam and corresponds to $x = \sin \Phi$. The maximum value of S_2 will occur if there are sharp Bragg peaks that are observed only at $\Phi = 90°$ and $\Phi = 270°$. This selection of a director is different from those of needle-like and cylindrical particles where the selection of a unique direction along a cylindrical axis would lead to different calculations of order parameters that describe the alignment of their unique particle axis with respect to the flow direction and corresponds to $x = \cos \Phi$.

Our diffraction measurements provide $I(\Phi)$ for various points in the flow. Order parameters, S_n, can be calculated readily from the data as in eq 1

$$S_n = \frac{\int_{\Phi=0}^{2\pi} I(\Phi) \mathrm{P}_n(\Phi)\, \mathrm{d}\Phi}{\int_{\Phi=0}^{2\pi} I(\Phi)\, \mathrm{d}\Phi} \qquad (1)$$

The integrals simply provide the normalized averages that were described above. Computationally, the integrals are evaluated numerically as a weighted sum of the data around the ring of a given diffraction peak. Equation 1 is analogous to the calculation of a correlation coefficient between the data and simple angular distributions. Values of S_2 calculated from the experimental data for different vertical positions in the pipe are shown in Figure 7.

Figure 7 indicates that there is almost complete alignment of particles near the wall of the pipe (S_2 about 0.9). At the center of the pipe, a large fraction of the particles have no preferential orientation (S_2 about 0.3). These wall effects were also observed in our previous work.[10] Towards the center of the pipe, the value of S_2 decreases. The higher value of S_2 suggests that more particles are aligned with their 001 normal orthogonal to the flow direction. The values of S_2 at both ends are similar, which shows that the particles keep their order in the direction of flow as they move along the straight pipe. Particles assemble and form an ordered layer of ~0.2 mm at the wall in the whole pipe. The shift in the data points for the inlet and outlet shown in Figure 7 is similar to that in Figure 6b and arises from the tilted mounting of the pipe.

Using eq 1, it is possible to calculate order parameters S_n for arbitrary n. P_4 has peaks at 0°, 90°, 180°, and 270° (shown in Figure S1 in the Supporting Information) and the value of S_4 is therefore useful to identify biaxial orientation. In the present experiments for flow along a straight pipe, this is not very useful. Odd Legendre polynomials could also be used as order parameters. These functions are antisymmetric and thus may be used to identify other features in the data, for example, tilt away from a principal axis.

Comparison with Fluid Mechanics Simulations. A finite-element computation package, *COMSOL Multiphysics*,[33] was used to make a simple simulation of the flow in the pipe. In an iterative procedure, the software calculates the flow patterns in defined geometries and with boundary conditions such as fluid velocity at the inlet and outlet points. The sample is modeled with a constant viscosity. Although it is not possible to include a detailed constitutive equation that would describe the changes in the rheological properties with shear rate and at high volume fraction, these are not required for the present comparison. The particle volume fraction was taken as 0.032, corresponding to the sample used, and thus, the viscosity is only slightly greater than that of pure water. This sample does not show significant shear thinning. Simulations were, as expected, insensitive to small changes in the particle volume fraction or particle size when included. The simulations assumed no slip boundary conditions at the wall of the pipe. Simulations of concentrated dispersions can be made using Brownian dynamics, but these were not necessary for the comparison with a sample at low volume fraction and almost constant viscosity. Such methods have been used for plate-like particles but are computationally demanding.[34]

Average flow velocities for the inlet and outlet regions were calculated to be 1.3 m s^{-1} from the measured overall flow rate. The derivative, dv/dR, of the local velocity, v, in the radial direction across the pipe gives an estimate of the shear strain rate. The average values of shear-strain rate along chords in the Y direction were calculated from the radial velocity profiles that were averaged over a 10 mm length between $X = 40$ and $X = 50$ mm. These are shown in Figure 8 for points from the center to the edge of the pipe. As the scattering experiment provides data that are averaged along a chord for the sample, equivalent averaging is made for the strain rate. If the beam passes through the center of

(33) *COMSOL Multiphysics* v 3.5a: http://www.comsol.com/
(34) Meng, Q.; Higdon, J. J. L. *J. Rheol.* **2008**, *52*, 1–36.

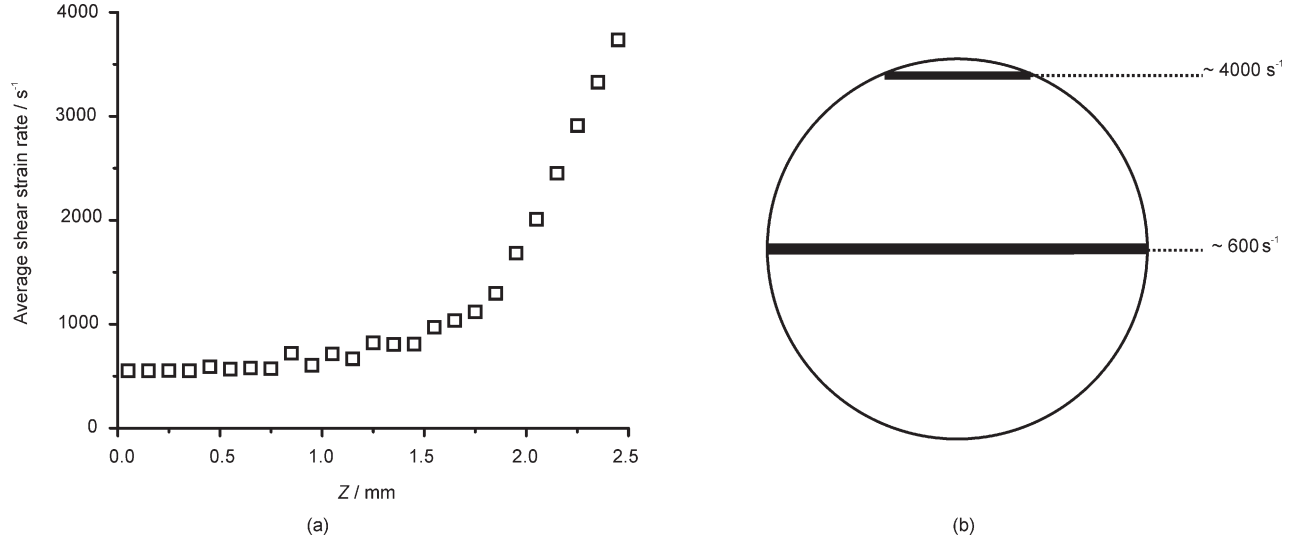

Figure 8. The strain rate calculated from finite element simulations of the velocity of a flowing dispersion in a straight pipe are shown in (a) as average values along chords at different distances, Z, from the center of the pipe. This chord averaging of the strain rate in the radial direction is illustrated schematically in (b).

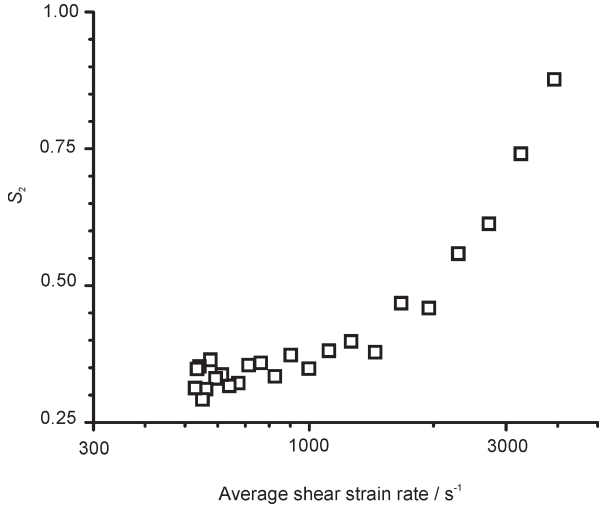

Figure 9. Values of orientation distribution function, S_2, are plotted against the average shear-strain rate in a pipe. S_2 increases from the center of the pipe to the wall as the shear strain rate increases.

the pipe, it will traverse regions with a full range of strain rates from zero at the center to the maximum at the wall, and for a beam near the edge of the pipe, only high shear rates are sampled.

Details of the flow profiles from the simulations are shown in the Supporting Information [S4]. A comparison of the experimentally determined values of the order parameter S_2 with the simulated average shear-strain rate is shown in Figure 9.

The orientational order of the particles is seen to increase markedly as the average strain rate increases beyond 1000 s^{-1}. A useful parameter in considering shear flow is the dimensionless quantity known as the Peclet number,[1] P_e, that is defined as

$$P_e = 6\pi\eta a^3(d\gamma/dt)/k_B T \quad (2)$$

where a is a characteristic length of the particles in a fluid of viscosity η, $d\gamma/dt$ is the shear-strain rate, k_B is Boltzmann's constant, and T is the absolute temperature. For the particles of diameter 1 to 2 μm, P_e is about unity at 1000 s^{-1}. As expected when Pe is greater than unity, which corresponds to shear-strain energies larger than the thermal energies for the particles, orientational order measured by S_2 is seen to increase. The transition would be broader if the particles were more polydisperse in size.

Values of S_2 are averaged for the same position on the opposite sides of the axis across the pipe along Z direction by considering the axis of the pipe is at $Z = 0$ mm. The plot in Figure 9 shows that the alignment increases as the shear-strain rate increases from the center to the wall in a cylindrical pipe. Measurements at a single flow rate allow data to be collected for a wide range of average shear-strain rates. Lower flow rates would not be expected to show any orientation. Higher flow rates can give rise to other effects such as turbulence.

Outlooks. In principle, tomographic analysis would be attractive, but this presents several geometrical problems in this type of experiment. Measurements with the beam traversing the sample at different angles would determine averages with more complicated paths of shear flow. It is not possible to measure with the beam parallel to the flow direction. Rectangular section pipes provide some advantages as the gradients in flow velocity can be very different in two directions. Tomographic analysis is still difficult, and the sample thickness cannot be optimized for both dimensions of the pipe. Dispersions with a higher volume fraction of particles and consequently that have more complicated rheology with effects such as shear thinning would be interesting to study and are readily accessible for this type of experiment. Detailed interpretation would require comparison with realistic computer models of the microstructure of the colloidal dispersion such as those based on Brownian dynamics simulations.

Conclusions

We have demonstrated the use of a recently developed technique that uses angle-dispersive high-energy X-ray diffraction to study flow of complex fluids. The experiments show the advantages over other complementary techniques. High-energy X-rays have a low absorption coefficient and thus penetrate thick samples and containers. Two-dimensional detectors allow data collection simultaneously over a range of Bragg angles and orientation directions. Translation of the sample in one, two, or three dimensions allows mapping of sample composition and the orientation of diffracting particles with spatial resolution of the order of 50 μm.

Dispersions of kaolinite particles (average diameter ca. 1 μm and thickness less than 0.05 μm) were studied under flow in a uniform cylindrical pipe. The particles were seen to align with their plate normals perpendicular to the direction of flow and they retain their alignment as they flow down the pipe. However, strong alignment effects were observed within 0.2 mm of the walls. The strongly aligned region of the sample showed a Lorentzian distribution of orientations of the particles. This could be resolved in these measurements, whereas previous studies with energy-dispersive X-ray and neutron diffraction were limited to the use of much larger beam sizes and thus averaged over large regions of the flow pattern.

Although the technique described can obtain the complete orientation distribution of particles, a straightforward technique has been presented to evaluate order parameters that are directly comparable with the results of other measurement techniques such as optical birefringence or nuclear magnetic measurements. Order parameters obtained from the coefficients, S_n, of a series of Legendre polynomials provide quantitative information about the alignment of particles in the flow. For the flow in the straight pipe, the value of S_2 that provides an average measurement of the orientational alignment is very high near the wall, 0.9, and reduces to 0.3 at the center of the pipe.

Simple computer simulations for a dispersion of particles under conditions of pipe flow provide a means to compare the alignment with the local velocity distribution in the flow field. The extent of orientation correlates well with the average shear-strain rate and increases noticeably above 1000 s^{-1} for the sample studied. This corresponds to Peclet numbers larger than unity for which orientational alignment would be expected to occur.

The aluminum used for the pipe is not optimal in all aspects. The large grain size gives rise to secondary diffraction that appears irregularly in the measured data. Other materials such as amorphous polymers have the advantage of no diffraction but can suffer from distortion at the pressures required for practical studies.

The technique can be readily extended to other geometries of flow and a range of different samples. For example, fundamental studies of colloid rheology benefit from a pipe with a rectangular cross-section to avoid the complexity of averaging over a cylindrical flow pattern. It is also possible to study more complex flow geometries such as those of engineering interest: this technique has been applied to the study of a pipe with a nozzle constriction as will be discussed in a later article.

Acknowledgment. We are grateful to the ESRF, Grenoble for the allocation of beam time. We also thank Jonathan Targett for assistance during the measurements.

Supporting Information Available: Experimental details and the data analysis procedures are described. The first three even Legendre polynomials and how their average values relate to order parameters are shown. Simulation results for the velocity profile across the pipe averaged along chords at different positions are provided. This material is available free of charge via the Internet at http://pubs.acs.org.

Alignment of plate-like particles in a colloidal dispersion under flow in a uniform pipe studied by high-energy X-ray diffraction

Supporting Information

S. Junaid S. Qazi, Adrian R. Rennie, Jonathan P. Wright, Jeremy K. Cockcroft

S1. Experimental Details

(a) Diffractometer

The ID11 beam line at ESRF, Grenoble is equipped with an in-vacuum undulator, which gives total integrated flux of about 10^{16} photons s^{-1} at high X-ray energies[1]. A monochromatic beam is obtained from a Si (111) monochromator with mirrors for harmonic rejection. The data were recorded with a Bruker "Smart 6500" 2048 × 2048 pixel CCD area detector placed at about 1.4 m from the sample. The effective pixel size was approximately 0.15 mm × 0.15 mm. This provides data over a range of diffraction angles up to about 6.5° in 2θ.

(b) Flow and Data Acquisition

Flow through the cylindrical pipe was maintained using a centrifugal pump (Totton Pumps, Model GP40/6). The pump was driven by a magnetically coupled, variable speed A.C. motor. Varying the applied voltage allowed different flow rates to be selected. The pump was connected by silicone elastomer tubing to the aluminum pipe and the outlet was connected to a reservoir that was used to feed the pump in a closed cycle. A total sample volume of about 600 mL was used.

Scans were made across the pipe by moving the pipe vertically in steps of 50 μm through the beam. Each point was measured for 60 s.

[1] ID11 beam line: http://www.esrf.eu/UsersAndScience/Experiments/StructMaterials/ID11

S2. Data Reduction

It is necessary to exclude the single-crystal aluminum diffraction peaks from the I(Φ) data. Some of these Bragg peaks are superimposed on the rings of clay diffraction intensity or the neighboring background. As multiple diffraction peaks from the grains are almost randomly distributed on the detector, these peaks cannot be subtracted by the simple algorithm described above. As mentioned the peaks depend on the grain structure of the pipe and thus vary between individual frames measured at different positions. The characteristic feature of this scattering from aluminum is that there is very high intensity in small regions on the detector. The Bragg scattering from the kaolinite is smoothly varying with the azimuthal angle and so a simple statistical algorithm was developed to mask pixels from analysis that contained significant aluminum diffraction. Different values of the discrimination limits were tested and it was found that the aluminum scattering was well eliminated when adjacent pixels in I(Φ) that differ by more than three standard deviations from the diffracted intensity of the kaolinite that was estimated from counting statistics are excluded from subsequent analysis.

S3. Legendre polynomials

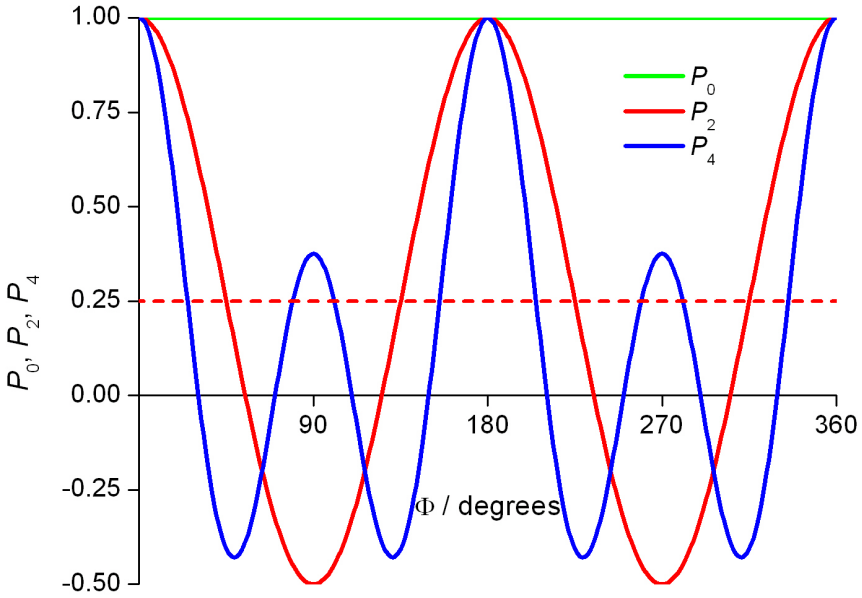

Figure S1. Legendre polynomial P_0, P_2, and P_4 are shown. The average value of P_2 is 0.25 and is indicated by the dashed line.

The order parameter S_2 in the main article is based on P_2. A fully aligned sample with all diffracted intensity in a single direction would have a value of S_2 equal to maximum of P_2 (i.e. 1.0). When there is no preferential order, S_2 takes the average value of P_2, which is 0.25.

S4. Simulations

The averaged velocity profile obtained from the simulation of the flow in the pipe is shown.

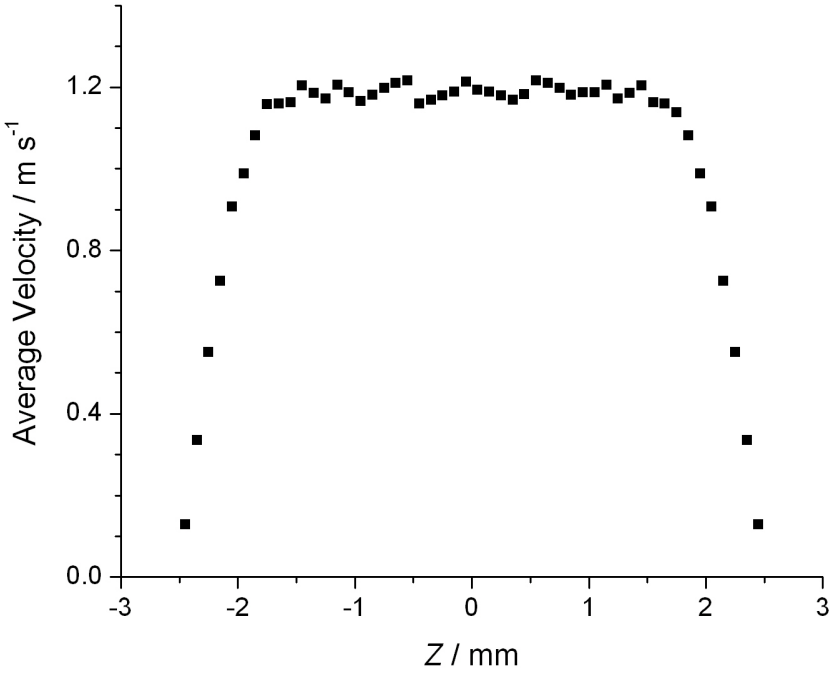

Figure S2. Chord-averaged velocity profile across the pipe that is obtained from the fluid dynamics simulations is shown.